

Wake/shear layer interactions in the low-Reynolds-number flow over multi-element airfoil

Jiangsheng Wang¹, Jinjun Wang^{1*} and Tian Li^{1,2}

¹ Beijing University of Aeronautics and Astronautics University, Key Laboratory of Fluid Mechanics
(Ministry of Education), Beijing, China

² Shenyang Aircraft Design and Research Institute, Shenyang, China

*jjwang@buaa.edu.cn

Abstract

Different kinds of wake/shear layer interactions for low-Reynolds-number flow over multi-element airfoil (30P30N) are observed with time-resolved particle image velocimetry (TR-PIV) and hydrogen bubble visualization. The Reynolds numbers based on the stowed chord length (Re_c) range from 9.3×10^3 to 3.05×10^4 . According to the hydrogen bubble visualization, the slat wakes can be divided into two types by a critical interval of Reynolds number ($1.27 \times 10^4 < Re_c < 1.38 \times 10^4$). These two kinds of slat wakes could interact with the shear layer above the main element in different ways. While Re_c is smaller than this critical interval, Görtler vortices dominate the slat wake and could induce streaky structures within the separated shear layer above the main element. While Re_c is larger than this critical interval, spanwise vortices and streamwise vortices co-exist in the slat wake. The boundary layer on the main element is more receptive to the spanwise vortices in the gap region to generate spanwise “double-secondary vortices”.

1 Introduction

The low-Reynolds-number flows have been explored widely to meet the development of small aerial vehicles. However, these investigations mainly focus on single-element airfoils or simplified flat plate models. As high-lift configurations, multi-element airfoils have shown satisfactory aerodynamic performance at high Reynolds numbers ($Re_c = 10^6 \sim 10^7$) (Van Dam 2002). Unfortunately, these high-lift configurations are relevant contributors to the airframe noise. To optimize the aerodynamic performance and reduce the aeroacoustics noise, the high-Reynolds-number flow related to multi-element airfoils has been investigated extensively. However, the low-Reynolds-number flow over this kind of configuration is still an open issue. Progress in this issue could further deepen the understanding of low-Reynolds-number flow and finally stimulate the development of small aerial vehicles. The complex geometry of multi-element airfoil results in the inherent interactions between the wake of one element and the boundary layer of the downstream element (Squire 1989). The current work will focus on the interactions between the slat wake and the shear layer above the main element at low Reynolds numbers.

Coherent vortices prevail in the slat wake of both the high-Reynolds-number flows and the low-Reynolds-number flows. For the high-Reynolds-number flows, the classical particle image velocimetry (PIV) results indicated that shed spanwise vortices dominated the slat wake (Jenkins et al. 2004). Meanwhile, the three-dimensional zonal detached eddy simulation of Deck et al. (2013) hinted the coexistence of streamwise vortices and spanwise vortices in the slat wake. For the low-Reynolds-number flows, the absolute instability of the laminar slat wake and the acoustic feedback between the slat boundary layer and the

trailing-edge noise resulted in the slat wake dominated by shed spanwise vortices in $8.4 \times 10^4 < Re_c < 2.1 \times 10^5$ and $2.1 \times 10^5 < Re_c < 5.9 \times 10^5$, respectively (Makiya et al. 2010). Wang et al. (2018) observed that streamwise vortices called Görtler vortices dominated the slat wake at $Re_c = 8320$ and $\alpha = 2 \sim 12^\circ$. The upper right boundary of the separation bubble in the slat cove (virtual curved boundary) could play the role as a real curved wall to produce Görtler vortices.

The coherent vortices in the slat wake could potentially interact with the boundary layer of the main element. The interactions between wake vortices and boundary layers have been explored extensively with the simplified configuration, which usually contains a circular cylinder to generate wake vortices and a flat plate to provide boundary layer. For the case of cylinder in the upstream and above the plate, previous hot-wire measurements and numerical simulations respectively captured the prevalence of spanwise secondary vortices (Kyriakides et al. 1999) and streamwise streaky structures (Ovchinnikov et al. 2006) within the boundary layer, as the response to cylinder wakes. Different flow structures with similar configurations was explored by Pan et al. (2008), it was clearly observed with hydrogen bubble visualization that the spanwise secondary vortices were generated inside the boundary layer with an “one-to-one” correspondence to wake vortices. These spanwise secondary vortices could evolve into hairpin-like vortices and finally contributed to the self-sustained turbulent boundary layer. In order to avoid the potential complex leading-edge receptivity in this cylinder-plate configuration, He et al. (2013) conducted PIV measurements and hydrogen bubble visualizations for the cylinder downstream of the leading edge of the flat plate. Spanwise secondary vortices induced by the wake vortices still existed in the boundary layer. Furthermore, the formation of secondary vortices was characterized by an exponential growth. The wake disturbances with the frequency of vortex shedding directly penetrated into the boundary layer and were amplified by an exponential growth, which finally led to the spanwise secondary vortices with the same frequency as the vortex shedding. The growth of low-frequency disturbances inside the boundary layer could be attributed to the three-dimensional destabilization of the secondary vortices, from spanwise vortices to hairpin-like vortices. Subsequently, He et al. (2016) investigated the evolution of Lagrangian coherent structures in the wake-induced boundary layer transition. At the beginning of transition, the spanwise wavelength of the deformed secondary vortices agreed with that of the deformed wake vortices. This agreement indicated that the three-dimensional instability of the secondary vortices was stimulated by the three-dimensional disturbances of the wake. Though progress has been made with simplified configurations, the interactions between wake vortices and boundary layers still need further explorations, especially in complicated configurations related to engineering practice (as the multi-element airfoil in the current work). Previous work found that the Görtler vortices in the slat wake could interact with the separated shear layer above the main element and induced streaky structures within the separated shear layer (Wang et al. 2018). In the current work, more results with Reynolds numbers larger than Wang et al. (2018) (from 9.3×10^3 to 3.05×10^4) are provided to reveal the effects of Reynolds number on the wake/shear layer interactions for flow over multi-element airfoil.

2 Experimental setups

The multi-element airfoil (30P30N) investigated in the current work is a scaled model of AIAA BANC-II Workshop (Choudhari et al. 2012). This airfoil has the same size and installation as the previous work with a 150 mm stowed chord length and a 500 mm span (Wang et al. 2018). The definitions of the angle of attack and the coordinate system are also the same with the previous work. The experiments are conducted in the water tunnel of the Institute of Fluid Mechanics at the Beijing University of Aeronautics and Astronautics. The free stream velocities U_∞ are varied from 62 mm/s to 204 mm/s, resulting in $Re_c = 9.3 \times 10^3 \sim 3.05 \times 10^4$. The free stream turbulence intensities are less than 0.8% in all the test cases. As the previous work done by Wang et al. (2018), $\alpha = 4^\circ$ is still the focus of the current work.

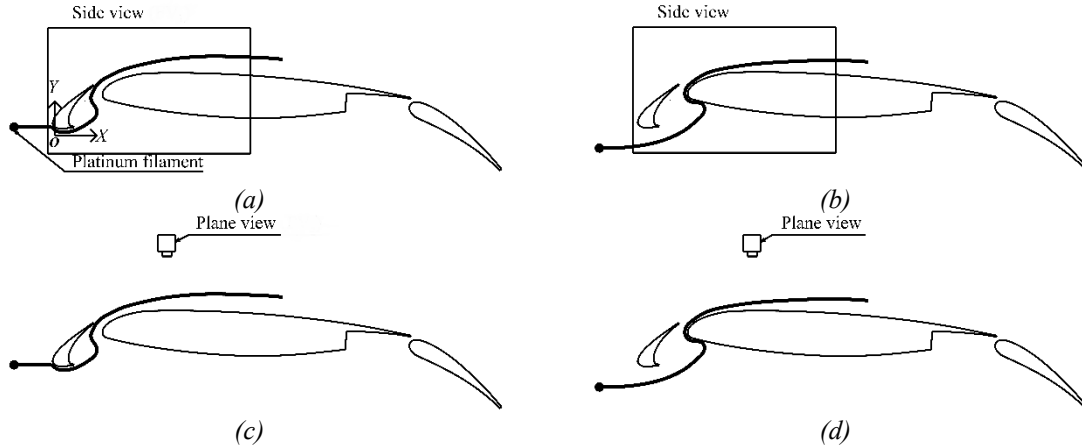


Figure 1: Sketch of hydrogen bubble visualization.

Hydrogen bubble flow visualization is conducted to provide the qualitative information of the flow. The sketches of experimental set-up for visualization are depicted in figure 1. A hydrogen bubble curtain is generated from a horizontal platinum filament upstream of the slat. The horizontal platinum filament can be adjusted in the vertical direction to make the curtain respectively strike the forward stagnation point of the slat and the main element before passing through the gap region. The setups of figure 1(a) and 1(c) are used to visualize the flow structures in the slat wake. The setups of figure 1(b) and 1(d) are used to visualize the flow structures above the main element. For the side view measurements (figure 1a,b), two vertical laser sheets, generated from two semiconductor continuous lasers (8-W, 532 nm), are co-operated to simultaneously illuminate the gap region with complex geometry. The streaky line illuminated by the laser sheet is recorded by a CMOS camera. The sampling frequencies of the CMOS camera are varied from 100 Hz to 250 Hz with Re_c . A CMOS camera combined with a volume illumination is utilized for the plane view measurement (figure 1c,d). The sampling frequencies of the CMOS camera are varied from 100 Hz to 300 Hz with Re_c . Two-dimensional time-resolved particle image velocimetry (TR-PIV) is utilized to provide the quantitative information of the flow. The setups of the CMOS camera and the laser sheets are similar to the side view flow visualization (figure 1a). Hollow glass beads with a median diameter of 10 μm are used as tracer particles. The sampling frequencies of the CMOS camera are varied from 250 Hz to 800 Hz with Re_c . Velocity fields are obtained by the Lucas-Kanade algorithm (Pan et al. 2015). Both the Multi-grid iteration with window deformation and the sub-pixel interpolation are contained in this algorithm to improve the velocity field. The interrogation window sizes of the final pass are set to be 32×32 pixels with overlaps of 75% in all test cases.

3 Hydrogen bubble visualization results

For $9.3 \times 10^3 < Re_c < 1.27 \times 10^4$, no roll-up or vortex shedding related to the slat cusp shear layer is observed in the gap region. A typical scenario is shown in figure 2(a). The slat cusp shear layer reattaches to the slat trailing edge with a laminar state. The upper right boundary of separation bubble in the slat cove works as a stable instantaneous virtual curved boundary to generate Görtler vortices (figure 2b). As a result, Görtler vortices dominate the slat wake within this Re_c regime. While for $1.38 \times 10^4 < Re_c < 3.05 \times 10^4$, the roll-up resulted from K-H instability occurs to the slat cusp shear layer. A typical scenario is shown in figure 2(c). The roll-up is followed by the shed spanwise vortices, which are deformed by the accelerated gap flow to form “hairpin-like” vortices in the slat wake (figure 2d). The heads of hairpin-like vortices still possess coherence in the spanwise direction (marked by the red line in figure 2d). The legs of hairpin-like vortices are visualized as counter-rotating streamwise vortices in figure 2(d) (marked by red boxes). As a result, spanwise vortices and streamwise vortices co-exist in the slat wake within this Re_c regime.

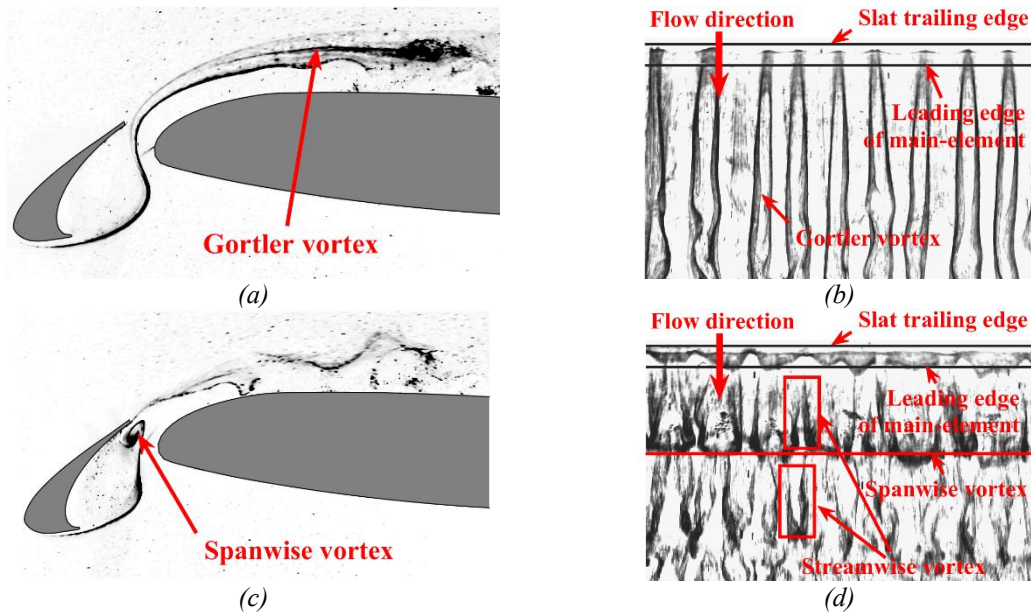


Figure 2: Hydrogen bubble flow visualization of slat wake. (a) side view, $Re_c=1.27 \times 10^4$; (b) plane view, $Re_c=1.27 \times 10^4$; (c) side view, $Re_c=1.83 \times 10^4$; (d) plane view, $Re_c=1.83 \times 10^4$.

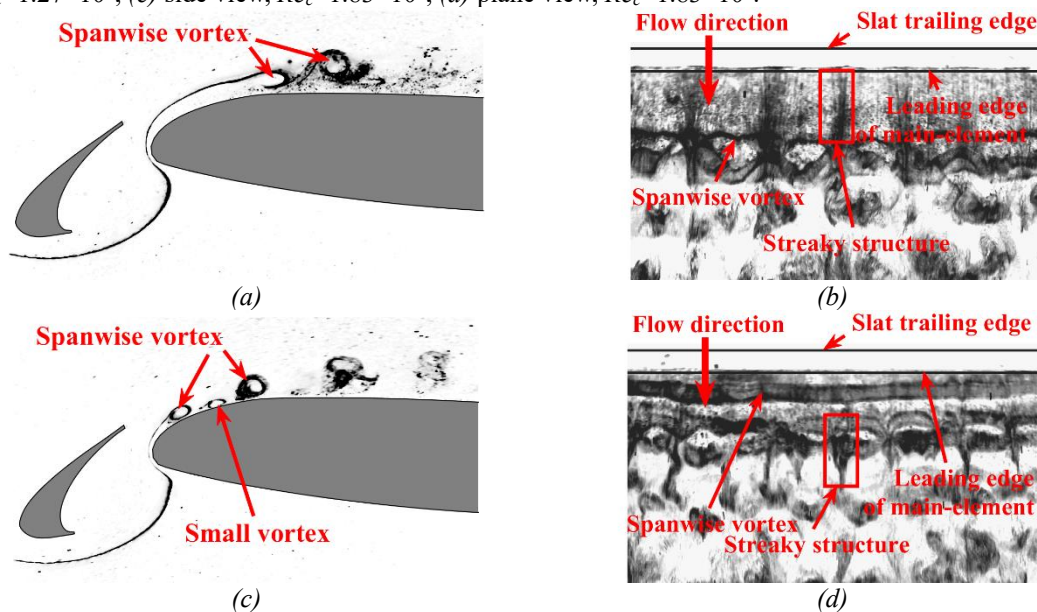


Figure 3: Hydrogen bubble flow visualization of the shear layer of main element. (a) side view, $Re_c=1.27 \times 10^4$; (b) plane view, $Re_c=1.27 \times 10^4$; (c) side view, $Re_c=1.83 \times 10^4$; (d) plane view, $Re_c=1.83 \times 10^4$.

In the cases that Görtler vortices dominate the slat wake ($9.3 \times 10^3 < Re_c < 1.27 \times 10^4$), the leading-edge separation of the main element results in the separated shear layer above the main element, followed by the spanwise vortex shedding (typical results are shown in figure 3a). Streaky structures are captured in the leading-edge separated shear layer (marked by red box in figure 3b). In this Re_c regime, the flow characteristics above the main element are similar to the previous results at $Re_c=8.32 \times 10^3$ (Wang et al. 2018). Spanwise vortex shedding is still captured above the main element when the slat wake is dominated by both the spanwise vortices and the streamwise vortices ($1.38 \times 10^4 < Re_c < 3.05 \times 10^4$). The typical scenario is shown in figure 3(c). These spanwise vortices are convected downstream along the curved surface of the main element and finally suffer from vortex breakdown. Plane view results reveal the good two-dimensionality of these spanwise vortices (figure 3d). It should be emphasized that there is a small

spanwise vortex (marked in figure 3c) existing between two spanwise vortices with large scales in this Re_c regime.

3 Particle image velocimetry results

Compared to the local and qualitative results of the hydrogen bubble visualization, PIV results are employed to provide the quantitative information of the whole flow field. Cases at $Re_c=1.27\times 10^4$ and $Re_c=1.83\times 10^4$ are still taken as representative ones to illustrate the effects of different slat wakes on the shear layer above the main element. The velocity sequences related to the vortex shedding above the main element are extracted for phase identifications (Pan et al. 2013). Finally, the phase-averaged vorticity contours are shown in figure 4. For the case that Görtler vortices dominate the slat wake (figure 4a), no vortex shedding occurs around the gap region and the blunt slat trailing edge. The shed vortices originated from the K-H instability of the leading-edge separated shear layer are convected downstream periodically. While for the case that spanwise vortices and streamwise vortices co-exist in the slat wake (figure 4b), one shed spanwise vortex within the gap region could induce two spanwise vortices above the main element. Therefore, these spanwise vortices above the main element are defined as “double-secondary vortices”.

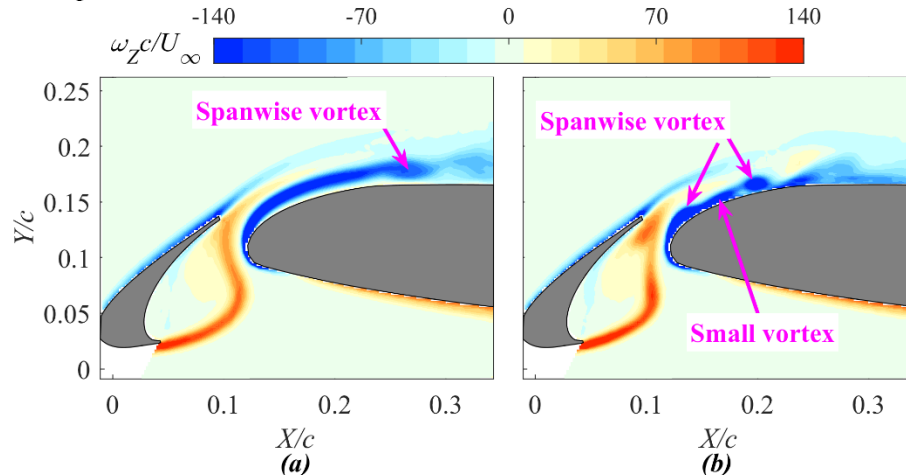


Figure 4: Vorticity contours of phase-averaged results. (a) $Re_c=1.27\times 10^4$; (b) $Re_c=1.83\times 10^4$.

4 Conclusion

Different kinds of wake/shear layer interactions in the low-Reynolds-number flow over multi-element airfoil (30P30N) are investigated with time-resolved particle image velocimetry (TR-PIV) and hydrogen bubble visualization. A critical interval of Re_c from 1.27×10^4 to 1.38×10^4 is found where the dominate flow structures change. The effects of slat wake on the shear layer above the main element can be divided into two types by this critical interval:

- (i). While Re_c is smaller than this critical interval, Görtler vortices generated from the virtual curved wall dominate the slat wake. These Görtler vortices reside above the separated shear layer of the main element and induce streaky structures within this separated shear layer.
- (ii). While Re_c is larger than this critical interval, the shed spanwise vortices originating from the K-H instability of the slat cusp shear layer prevail in the gap region. These spanwise vortices suffered from three-dimensional instability and then are deformed by the accelerated gap flow to form “hairpin-like” vortices in the slat wake. As a result, spanwise vortices (heads of hairpin-like vortices) and streamwise vortices (legs of hairpin-like vortices) co-exist in the slat wake. The spanwise vortices in the gap region could induce novel “double-secondary vortices” in the boundary layer of the main element, similar to the wake-induced “secondary vortices” with simplified configurations.

The present work could promote the research from simplified configurations to complicated

configurations related to engineering practice. However, the wake/boundary layer interactions still need to be explored for the flow over multi-element airfoil with higher Reynolds numbers ($Re_c > 10^5$).

Acknowledgements

This work is supported by the National Natural Science Foundation of China (11721202).

References

- Choudhari, M. M. and Yamamoto, K. (2012). Integrating Cfd, Caa, and Experiments Towards Benchmark Datasets for Airframe Noise Problems. *NASA Conference Paper* NF-1676L-14832
- Deck, S. and Laraufie, R. (2013). Numerical Investigation of the Flow Dynamics Past a Three-Element Aerofoil. *Journal of Fluid Mechanics* 732: 401-444.
- He, G.-S., Pan, C., Feng, L.-H., Gao, Q. and Wang, J.-J. (2016). Evolution of Lagrangian Coherent Structures in a Cylinder-Wake Disturbed Flat Plate Boundary Layer. *Journal of Fluid Mechanics* 792: 274-306.
- He, G., Wang, J. and Pan, C. (2013). Initial Growth of a Disturbance in a Boundary Layer Influenced by a Circular Cylinder Wake. *Journal of Fluid Mechanics* 718: 116-130.
- Jenkins, L. N., Khorrami, M. R. and Choudhari, M. (2004). Characterization of Unsteady Flow Structures near Leading-Edge Slat: Part I. Piv Measurements. *AIAA paper* 2801: 2004.
- Kyriakides, N. K., Kastrinakis, E. G., Nychas, S. G. and Goulas, A. (1999). Aspects of Flow Structure During a Cylinder Wake-Induced Laminar/Turbulent Transition. *AIAA Journal* 37(10): 1197-1205.
- Makiya, S., Inasawa, A. and Asai, M. (2010). Vortex Shedding and Noise Radiation from a Slat Trailing Edge. *AIAA journal* 48(2): 502-509.
- Ovchinnikov, V., Piomelli, U. and Choudhari, M. M. (2006). Numerical Simulations of Boundary-Layer Transition Induced by a Cylinder Wake. *Journal of Fluid Mechanics* 547: 413-441.
- Pan, C., Wang, H. and Wang, J. (2013). Phase Identification of Quasi-Periodic Flow Measured by Particle Image Velocimetry with a Low Sampling Rate. *Measurement Science and Technology* 24(5): 055305.
- Pan, C., Wang, J. J., Zhang, P. F. and Feng, L. H. (2008). Coherent Structures in Bypass Transition Induced by a Cylinder Wake. *Journal of Fluid Mechanics* 603: 367-389.
- Pan, C., Xue, D., Xu, Y., Wang, J. and Wei, R. (2015). Evaluating the Accuracy Performance of Lucas-Kanade Algorithm in the Circumstance of Piv Application. *Science China Physics, Mechanics & Astronomy* 58(10): 1-16.
- Squire, L. (1989). Interactions between Wakes and Boundary-Layers. *Progress in Aerospace Sciences* 26(3): 261-288.
- Van Dam, C. (2002). The Aerodynamic Design of Multi-Element High-Lift Systems for Transport Airplanes. *Progress in Aerospace Sciences* 38(2): 101-144.
- Wang, J.-S., Feng, L.-H., Wang, J.-J. and Li, T. (2018). Görtler Vortices in Low-Reynolds-Number Flow over Multi-Element Airfoil. *Journal of Fluid Mechanics* 835: 898-935.